International Journal of Mass Spectrometry 303 (2011) 55–62

Contents lists available at ScienceDirect

International Journal of Mass Spectrometry

journal homepage: www.elsevier.com/locate/ijms

Metastable dissociative decay of fluorofullerene negative ions

Rustem V. Khatymov[a,*], Pavel V. Shchukin[a], Renat F. Tuktarov[a], Mars V. Muftakhov[a], Vitaliy Yu. Markov[b], Ilya V. Goldt[b]

[a] Institute of Molecules and Crystals Physics, Ufa Research Center of Russian Academy of Sciences, Prospekt Oktyabrya, 151, 450075 Ufa, Russia
[b] Chemistry Department, Moscow State University, Leninskie gory 1-3, 119992 Moscow, Russia

ARTICLE INFO

Article history:
Received 4 October 2010
Received in revised form 6 December 2010
Accepted 22 December 2010
Available online 30 December 2010

Keywords:
Fluorofullerene
Resonant electron capture mass spectrometry
Autodetachment
Metastable negative ion
RRKM
Kinetic shift

ABSTRACT

In the course of the resonant electron capture mass-spectrometric study of the fluorinated fullerenes $C_{60}F_{18}$, $C_{60}F_{36}$ and $C_{60}F_{48}$, the processes of the metastable (slow, delayed) decay of negative ions by loss of fluorine atoms, effectively competing with electron autodetachment were detected. Theoretical analysis of the unimolecular decomposition, carried out on the basis of the statistical RRKM theory, showed that the excess of the appearance energy of fragment ions over the energy threshold results from a kinetic shift. It is shown that rapid processes of fragmentation of fluorofullerene molecular ions take place in addition to a metastable decay.

1. Introduction

Owing to wide variety of their unusual physical and chemical properties, fullerenes have recently started to find application in various fields of science, engineering and technology. The developments using fullerenes in solar energy and organic electronics are the most promising ones in terms of economic effect. Fullerene component embedded in the organic semiconductor materials is able to stabilize the states with charge separation, thereby increasing the efficiency of the electronic device [1,2]. This property of fullerenes is determined by their ability to effectively capture electrons originating in the region of a bulk heterojunction and retain them for a long time.

An important advantage of fullerenes in comparison with other materials is the ability to "adjust" the electronic properties of molecules (the energy of frontier orbitals) and increasing their solubility in polymer materials by virtue of chemical modification. In particular, it has recently been shown [3,4] that the fluorinated fullerene molecules are well suited as doping agents in organic electronics, because of their energy levels compared to C_{60} have an optimum location relative to the levels of doped polymeric materials.

The carbon cage of C_{60} is distinguished by extremely high mechanical strength, thermal and chemical stability, resistance to destruction by the electromagnetic radiation, electronic and atomic collision in a wide impact energy range [5]. In contrast to the strongly fixed carbon atoms in a cage, any atoms or functional groups attached to them have a lower binding energy and can easily be detached by the external action. Therefore, along with doubtless advantages, the use of fullerene exohedral derivatives in electronics can be coupled with a problem of structural degradation of these electrophilic agents, which, in turn, affects the life cycle of electronic devices.

Since the main function of fullerenes in organic electronics is capture and retention of the electrons, the study of fullerenes interaction with electrons in model gas-phase conditions represents the most adequate approach within the framework of designated problem. Electrons in the condensed phase are characterized by low kinetic energy. In the gas-phase conditions interaction of such electrons with the molecules leads to the so-called resonant capture with the formation of negative ions (NI). It has been previously established by the method of NI mass spectrometry, that molecules of C_{60} and C_{70} possess high resistance to fragmentation in the process of the resonant electron capture in a wide energy range from 0 to 14 eV and above [6]. In a similar study [7] of $C_{60}F_{48}$ fluorofullerene NI it has been shown, that fullerene cage decay does not occur even at energies 40 eV, and the most intensive channel of NI fragmentation is loss of F atom.

* Corresponding author. Tel.: +7 347 2848869.
E-mail addresses: LMSNI@anrb.ru, rustem@anrb.ru (R.V. Khatymov).

1387-3806/$ – see front matter © 2010 Elsevier B.V. All rights reserved.
doi:10.1016/j.ijms.2010.12.014

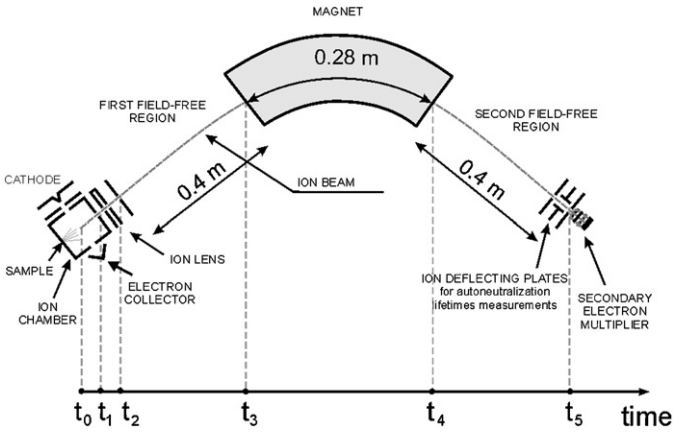

Fig. 1. Block diagram of the mass spectrometer showing the geometric dimensions and the time intervals of ions drift in the instrument (bottom).

This paper is devoted to study of the fragmentation processes of NI, formed by resonant electron capture by fluorofullerene molecules $C_{60}F_{18}$, $C_{60}F_{36}$ and $C_{60}F_{48}$. It is a logical extension of the investigation of NI decay by means of electron autodetachment (autoneutralization) [8]. At the achievement of definite electron energy (E_e) the most intense decay channel of molecular NI of fluorofullerenes becomes a loss of F atom; this channel strongly competes with the autoneutralization processes, and it will be subjected to detailed analysis from the viewpoint of the statistical RRKM theory.

2. Experimental

The experiments were performed using a magnetic sector mass-spectrometer MI-1201 (Sumy, Ukraine), modified to work with NI in the resonant electron capture mode. A survey of a resonant electron capture (REC) mass spectrometry method was published in Ref. [9,10]; the block diagram of a mass-spectrometric instrument is given in Ref. [11] and in a simplified form is given in Fig. 1 together with the geometric parameters of the device necessary to consider the kinetics of dissociative decay. The fluorofullerene samples synthesised by the known procedures [12–14], were deposited in advance directly on one of the inner walls of the ionization chamber made of stainless steel, and evaporated with a help of nichrome wire heater located outside of the chamber; the temperature was monitored with a thermocouple adjacent to the same wall. Briefly, the electrons emitted from a tungsten cathode and collimated by a field of the outer focusing electromagnet (B ~ 100 G) enter the ionization chamber and interact there with vapours of analyte. The ions thus formed are extracted from the ionization region, accelerated to the kinetic energy of 1.6 keV, and after passing the first field-free region of the mass spectrometer, are mass analyzed in the magnetic field of analyzer. Moving further, the ions of selected masses enter into the detector (secondary electron multiplier), from which the signal is amplified and transmitted to the recording computer. An instrument allows to record mass spectra by scanning the magnetic field at constant electron energy (E_e), and to register effective yield curves of NI as functions of E_e in the energy range 0–80 eV at constant magnetic field of the analyzer. The electron energy scale calibration was performed by the maximum of effective yield curves of SF_6^-/SF_6 (~0 eV); the full width at half maximum of this peak (*ca.* 0.6 eV) provided the estimation of the electron energy distribution in the vicinity of E_e scale beginning. In operation, the vapour pressure measured with an ionization gauge in immediate vicinity of the ionization chamber was in the range of 10^{-4} Pa, which corresponds to single-collision conditions.The fragment (daughter, D^-) ions generated during the dissociative decay of molecular (parent, P^-) NI within the ionization chamber (in the time interval t_0–t_1 in Fig. 1) are registered as a narrow mass-spectral peaks (with mass numbers m/z_{D^-} and m/z_{P^-}, respectively). At given geometry of mass-spectrometric system, that portion of fragment ions, which has formed due to later decay of parent ions after release from the ion source and during the drift in the first field-free region (in the time interval t_2–t_3) is detected as a diffuse peaks of metastable ions m*, with the apparent position of the maxima m/z_{m^*} in the mass spectrum determined by the simple relation $m/z_{m^*} = (m/z_{D^-})^2/m/z_{P^-}$ [15].

3. Results and discussion

Fig. 2a–c (upper panels) presents the NI mass spectra of the studied fluorofullerene samples obtained at $E_e \approx 0.15$ eV. Along with the intense peaks of molecular ions $C_{60}F_n^-$, n = 18, 36 and 48, the low intensity peaks of NI are exhibited in the mass spectra, corresponding to fluorofullerenes with an even number of fluorine atoms and their oxidized analogues. Judging from the mass-spectrometric data by laser-desorption methods [16], these weak peaks should be attributed to impurities. Further confirmation of the discussed peaks origin from the impurities are mass spectra [7] obtained under the similar experimental conditions for the sample $C_{60}F_{48}$ with other degree of purification and, consequently, somewhat different relative intensities of the observed peaks $C_{60}F_{40,42,44,46}^-$ with respect to the $C_{60}F_{48}^-$ peak intensity of target compound. In the low-energy mass spectra under discussion the peaks of ions with an odd number of F atoms are not observed. Also, in these experiments there were not revealed any ions formed by detachment of even number of F atoms from molecular NI, as well as F^- ions. This fact indicates to the absence of any fragmentation processes at thermal electron energies, or to the extremely low efficiency of such processes falling beyond the instrumental detection sensitivity. The observable fragmentation processes are beginning to appear at higher E_e, as evidenced by the mass spectra shown in the bottom panels of Fig. 2a–c. Along with the decreasing of relative intensity of the molecular ions peaks, the $C_{60}F_{n-1}^-$ (n = 18, 36, 48) peaks become dominant in these mass spectra. Other peaks of fragment NI, which are formed by the loss of a few F atoms, are detected as well.

A noticeable feature of high-energy mass spectra (Fig. 2, bottom panels) is the presence of diffuse metastable peaks m*, corresponding to the process (1) of the fluorine atom loss, occurring in a first field-free region of mass spectrometer:

$$C_{60}F_n^- \rightarrow C_{60}F_{n-1}^- + F \quad (1)$$

Fragment ions $C_{60}F_{n-1}^-$ produced at higher energies E_e are themselves subjected to a metastable fluorine atom loss during the drift of field-free region, which is evident by the presence of the peak m** with an apparent mass of 1005.96 amu in the $C_{60}F_{18}$ mass spectrum at E_e = 15 eV (Fig. 2a, bottom panel). This fact gives evidence of the multi-stage fragmentation processes in the fluorofullerene NI at high energies. A similar sequential dissociative decay of the trifluoromethylfullerene NI with elimination of the CF_3 units has been found previously [17]. In the present work a detailed consideration was carried out only for the first, most intense stage of dissociative processes (1), since other channels of molecular NI fragmentation are of low efficiency, which allows them to be neglected. Hereinafter, the ions $C_{60}F_n^-$ and $C_{60}F_{n-1}^-$ (n = 18, 36 and 48) formed in the ionization chamber are designated as P^- and D^-, respectively, and fragment ions $C_{60}F_{n-1}^-$ arising due to the process of P^- molecular NI decay in the first field-free region of mass spectrometer are denoted as m*.

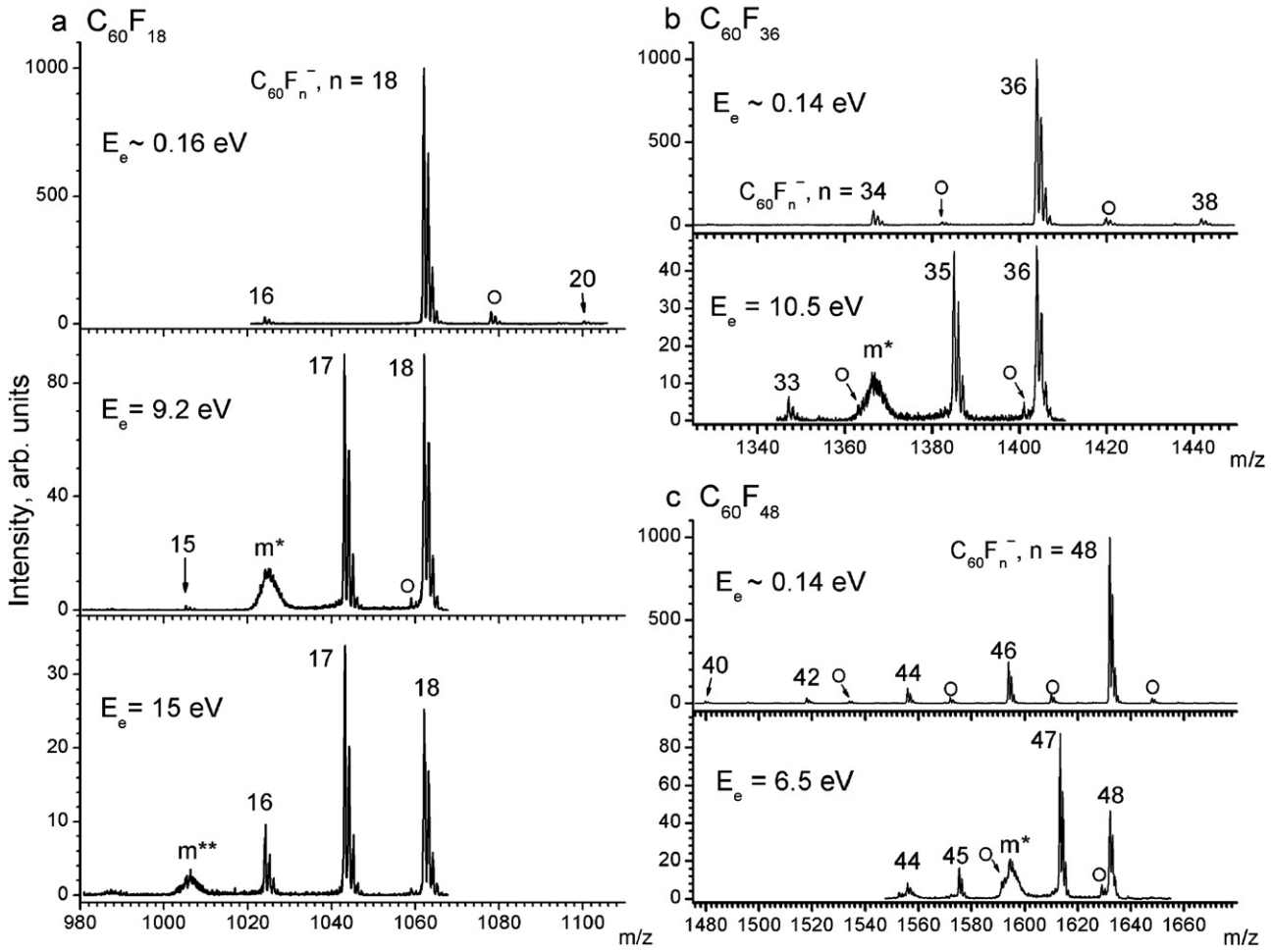

Fig. 2. Negative ion mass spectra of $C_{60}F_{18}$ (a), $C_{60}F_{36}$ (b) and $C_{60}F_{48}$ (c), recorded at thermal energy of captured electrons E_e (upper panels) and at energies E_e corresponding to the maximum yield of metastable ions m* and m** (see text; lower panels). The peaks of oxidized ions $C_{60}F_nO^-$ are marked by unfilled circles. The temperature of the ionization chamber while recording the mass spectra of (a)–(c) was 567, 445 and 420 K, respectively.

Fig. 3a shows the effective yield curves (EYC) of P^-, D^- and m* NI, as a function of E_e. For correct description of the unimolecular decay (1) the intensities of curves are normalized to the areas under respective mass peaks. It should be noted, that for P^- and D^- the areas of all peaks in the isotopic distribution (see Fig. 2) were incorporated; the insignificant contribution of $C_{60}F_{n-3}O^-$ ions was removed from the integral intensity of m* ions using the procedure analogous to that described in Ref. [8].

EYC of parent P^- and daughter D^- NI demonstrate a broad energy range of resonant electron capture by fluorofullerene molecules, partially covering the area of electron ionization of molecules (the threshold ionization energy of molecules $C_{60}F_n$ is 8.1 ± 1.0 eV [18], 11.06 ± 0.20 and 12.06 ± 0.20 eV [7] for $n = 18$, 36 and 48, respectively). The mechanisms responsible for electron capture by fullerene molecules in various E_e ranges have been discussed earlier [6,7,19]. In particular, the anomalous wide energy range of electron capture with consequent formation of long-lived fullerene molecular NI at nonthermal energies was explained by the excitation of collective (plasmon) oscillations in electronic shell of the molecules, which are believed to stabilize the high kinetic energy of impinging free electron [19,20]. The energy of such multielectronic excitations can be immediately transferred into nuclear vibrations what allows the system to bind extra-electron for a long time.

A sharp peak observed on the yield curves of the P^- ions at thermal energy and a gradual decrease in intensity with increasing E_e resembles the situation in long-lived C_{60}^-/C_{60} molecular ions [6]. However, the expansion of P^- curves to the higher-energy region is limited by fragmentation processes, as evidenced by the D^- yield curves serving as continuation of the former ones. The asymmetric and complicated shapes of D^- curves testifies to the contribution of several types of decay processes proceeding in the parent ions at different E_e and leading to the formation of D^-.

In contrast to the D^- curves, the m* curves have almost symmetrical shape without noticeable features. As noted above, m* represent the same daughter NI, but m* have been formed at a later time. Accordingly, the energy position of the m* peak varies from object to object in agreement with the main D^- peaks, without revealing, however, any correlation with the degree of fluorination of the fullerene. The maxima of m* peaks arrange just between P^- and D^- peaks, which agrees with Ref. [21] (this observation is an analogy with the appearance energies of parent, metastable and daughter positive ions in conventional mass spectrometry [15]).

In the most previously studied cases of resonant electron capture by the molecules of small size, the rapid fragmentation processes occur in NI (presumably for a time comparable with the vibrational period of interatomic bonds (nuclear vibration period)). This is due to strong competition with the processes of electron autodetachment [22]. For the molecular NI of C_{60}^- and its fluorinated derivatives it has been shown in a recent paper [8], that the lifetime with respect to electron autodetachment (τ_a) is a few hundred milliseconds, reaching at least one second range at

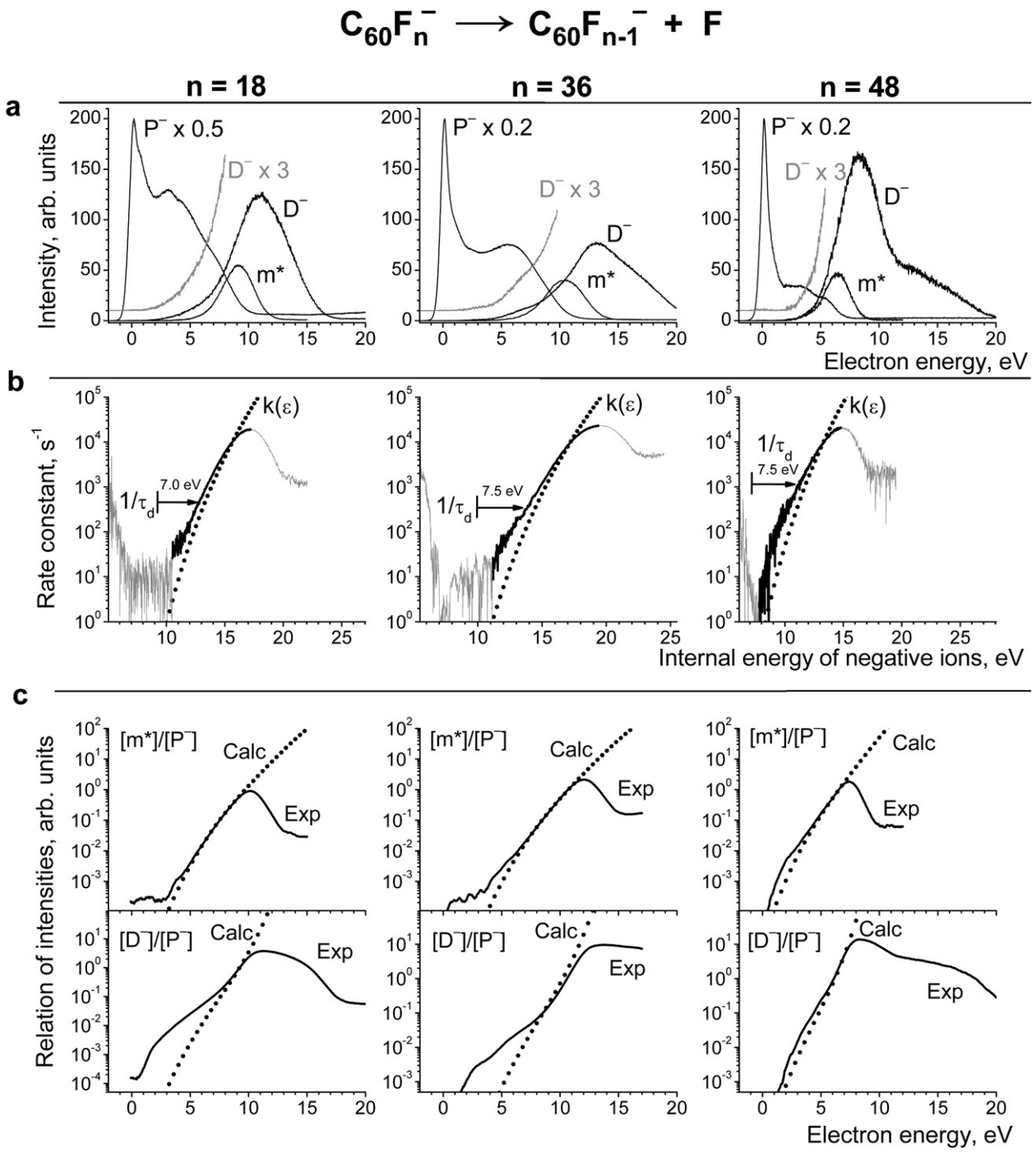

Fig. 3. Effective yield curves of the parent P^-, daughter D^- and metastable m* NI as a function of E_e (a); experimental curve of inverse dependence of NI lifetime with respect to dissociation $1/\tau_d$ versus E_e reduced to NI internal energy scale ε (solid line) (see text), and computed unimolecular decomposition rate constant $k(\varepsilon)$ (dotted line) (b); experimental (solid line) and calculated (dotted line) intensity relations [m*]/[P^-] and [D^-]/[P^-] as a function of E_e (c). The temperature of the ionization chamber in experiments with $C_{60}F_{18}$, $C_{60}F_{36}$ and $C_{60}F_{48}$ was 564 K, 475 K and 405 K, respectively.

thermal electron energy. Substantially long τ_a is a sufficient condition for a complete statistical redistribution of captured electron energy among the internal degrees of freedom of NI. Thus, it has been shown previously [23] on the example of C_{60} that autoneutralization of C_{60}^- NI has a statistical nature. Undoubtedly, such distinguishing feature as long τ_a of NI in the case of fullerene derivatives should be reflected on the character of their dissociative decay. Indeed, observed metastable (delayed in time) type of the NI fragmentation is another sure sign of relevance and applicability of the laws of statistical physics [15,21].

The most adequate and well-established theory in the mass spectrometry of positive ions is a statistical Rice–Ramsperger–Kassel–Markus theory (RRKM) [24,25]. In a number of reasons (see, e.g., Ref. [26]) RRKM is not widely accepted when considering the NI. Successful experience of applying this theory to the decay of negative ions by electron autodetachment [23] and by fragmentation [26] provides the basis of our choice of RRKM for describing the dissociative processes discussed in this paper. The statistical model proposed in Ref. [26] for the general case of *fragment* NI decay in competition with autoneutralization,

Table 1
Structural, energetic and temporal characteristics and parameters used to calculate relations [m*]/[P⁻] and [D⁻]/[P⁻] using the statistical RRKM model.

Decay scheme	$C_{60}F_n^- \rightarrow C_{60}F_{n-1}^- + F$				
	$n = 18$	$n = 36$		$n = 48$	
The symmetry of molecule	C_{3v}	C_3		D_3	
The electron affinity of molecule (EA_M), eV (from Ref. [16])	3.1	3.5		4.1	
Temperature of the ionization chamber (T), K	564	437	475	405	479
Vibrational energy of molecules ε_M, corresponding to the maximum of the Boltzmann distribution $f_M(\varepsilon)$, eV	3.9	3.4	4.0	3.39	4.7
Activation energy (E_a), eV	2.52	2.33		1.83	
Active frequency of the C–F bond, cm^{-1}	1165	1175		1178	
Reaction path degeneracy (σ)	18	36		48	
Full width at half maximum of electron energy distribution at $E_e = 0$ ($\Delta E_{1/2}(0)$), eV	0.59				
Factor of the broadening of electron energy distribution (a), eV/eV	0.1				
Moments of time t_1, t_2, t_3, and t_4 (see Fig. 1) at ions accelerating voltage of 1.6 kV, μs	17.2	20.3		21.3	
	17.2	20.3		21.3	
	40.0	47.3		50.1	
	56.0	66.2		70.3	

was adapted for the decay of *molecular* NI of fluorofullerenes (see Section 4). Appreciable simplification of the model was achieved at the expense of neglecting the abovementioned competition, what we have done from the following considerations. Assuming the exponential character of dissociative decay over time and using the effective yield curves of NI (Fig. 3a), we estimated the average lifetime of parent ions with respect to dissociation τ_d as a function of electron energy:

$$\tau_d \approx \frac{\Delta t_{FFR}}{\ln(1 + [m^*]/([P^-] + q[m^*]))},$$

where $\Delta t_{FFR} = t_3 - t_2$ is a time of P^- ions drift in the first field-free region (see Fig. 1 and Table 1) [m*] and [P⁻] are the numbers of detected metastable and parent ions (*i.e.*, intensities of recorded ion signals), $q = 0.7$ is a geometric factor of the device (the ratio of the length of ion path in the magnet region to the length of field-free region) (Fig. 3b shows the curves of the inverse dependence $1/\tau_d$.) The value of τ_d obtained in such a way is 0.1–1 ms at the energy of metastable m* peaks maxima, whereas autodetachment lifetime τ_a value for the $C_{60}F_n^-$ ions at the same energy region is 0.1–1 s [8].[1] Thus, fragmentation efficiency exceeds that of process of fluorofullerene NI autoneutralization on *ca.* 3 orders of magnitude, what allows not take into account the process of autoneutralization.

In accordance with the RRKM theory, the unimolecular reaction rate constant depends on a single experimental variable parameter—the ions' internal energy ε [24]. The estimation of this parameter for positive ions resulted from the electron ionization is a difficult task, because it depends on the energy carried away by removed electron in the process of ionization, moreover, this energy is not easy to measure experimentally [27,28]. In this connection, it should be emphasized that the internal energy of NI, formed by resonant capture of electrons with controlled energy, is well-defined quantity. Really, in a single collision conditions molecular NI inherit all the internal vibrational energy of neutral molecules ε_M, which was accumulated by them in the sample heated to a temperature of ionization chamber T, and electron capture leads to an increase of this energy by the value of electron affinity (EA) of the molecule plus the kinetic energy of captured electron: $\varepsilon = \varepsilon_M + EA + E_e$.

A detailed description of the procedures for calculating the value of ε_M, the function of decay rate constant and other model parameters are given in the Section 4. The function of decay rate constant $k(\varepsilon)$ versus ε is plotted in Fig. 3b in the same range of energies (covering 22 eV) as the effective yield curves (Fig. 3a), but biased to the value of $\varepsilon_M + EA = 7.0$, 7.5, 7.5 eV for $n = 18$, 36 and 48, respectively (see Table 1). This figure also shows the experimental curves $1/\tau_d$ (see above) versus electron energy E_e, reduced to the scale of the internal energy ε by simple shift to higher energies on the same amount $\varepsilon_M + EA$. Such a construction of the curves in Fig. 3b with respect to those in Fig. 3a provides an opportunity to see a clear coincidence of orders of magnitudes $1/\tau_d(\varepsilon)$ and calculated rate constant $k(\varepsilon)$ within the energy range of the efficient formation of metastable m* ions (see Fig. 3a). This allows one to make a preliminary conclusion about the correctness of the calculation of the function $k(\varepsilon)$.

Fig. 3c shows the experimental and calculated relation of intensities [m*]/[P⁻] and [D⁻]/[P⁻] depending on the energy of captured electrons. This manner of representing the effective yield curves allows to eliminate the resonant nature of electron capture and not to take into account in the calculations the unknown value of absolute NI formation cross sections [26]. Given that the single fitting parameter of the model was the magnitude a of the broadening of internal energy distribution of ions (see Section 4 and Table 1), and the value of the activation energy E_a was subjected to the insignificant correction, it should be noted a good coincidence between calculated and experimental relations [m*]/[P⁻] in a wide range of E_e, beginning from the appearance energy of m* ions up to the energy corresponding approximately to the middle of high-energy wing of this NI curves (compare with Fig. 3a).

The divergence of the experimental and calculated [m*]/[P⁻] curves at higher E_e, probably, is caused by increasing competition from the processes of P^- fragmentation by loss of more than one F-atom, as well as by growth of contribution from the processes of secondary electron capture, as indicated by the smoothly rising P^- curve in this area (see examples in Ref. [29]). In low-energy region the deviation of experimental curves is associated with another secondary process, namely collision activation by the residual gases, the contribution of which dramatically rises on the background of low signal to noise ratio at small m* ions yield. The same reasons are valid for the experimental $1/\tau_d$ curves demonstrating analogous behavior at low and high energy ranges (see Fig. 3b, the corresponding segments are highlighted by gray).

[1] It should be borne in mind that the measurement of τ_a was carried out in the ion detector region, *i.e.* in another time window than τ_d, however, this circumstance has virtually no effect on the results obtained.

The model curves $[D^-]/[P^-]$ for $C_{60}F_{48}$ calculated using the same parameters (Fig. 3c) show seemingly satisfactory agreement with experimental data. However, for the remaining two fluorofullerenes the more or less fair coincidence is observed only in a narrow energy region near the maxima. Singularities in the form of an inflection or shoulder can be detected at close examination of the low-energy wings of the yield curves of D^- ions from $C_{60}F_{18}$ and $C_{60}F_{36}$ (Fig. 3a) in the range from 2 to ≈8 eV. These singularities in the corresponding experimental relation curves $[D^-]/[P^-]$ (constructed on a logarithmic scale) cause a pronounced deviation from the calculated curves. Also, it is necessary to pay attention to the fact that fragmentation efficiency for $C_{60}F_{48}^-$ reaches its maximum at the capture of electrons with smaller energy as compared with $C_{60}F_{18}$ and $C_{60}F_{36}$, and in the corresponding D^- curve at $E_e \approx 8$ eV one can observe the main peak instead of shoulder.

A significant exaggeration of the $[D^-]/[P^-]$ experimental values over those predicted by the current model indicates to excessive efficiency of fragmentation occurring within the ionization chamber. It is logical to assume, that these "extraneous" decay processes are not described by the given statistical model due to the fact that they occur quite rapidly; at the time of entering of parent ion into the first field-free region, they have been practically completed, and therefore, do not make any noticeable contribution to the formation of m* ions.We attempted to find out the origin of these "extraneous" processes of fragmentation with a help of series of additional experiments:

(1) Recording the effective yield curves of NI at different values of the accelerating potential (800 V), *i.e.*, in another time window of measurements, revealed a slight displacement of curves $[m^*]/[P^-]$ (Fig. not shown), which is fully explained by the statistical model with an appropriate change of time parameters t_3–t_5. A shape of $[D^-]/[P^-]$ curves, in general, remains the same, except the region near maximum. These observations confirm the localization of the "extraneous" processes solely within the ionization chamber.
(2) The assumption of a possible catalytic activation of molecules by material of surface, from which the samples were evaporated, has not been confirmed. The data, obtained in the experiment with deposition of sample on a copper plate attached to the steel wall of the ionization chamber, have not shown any differences or distinctive features.
(3) One more our assumption was associated with a possible temperature gradient of the ionization chamber, which could lead to additional thermal activation of some portion of molecules of evaporated samples. To test this hypothesis, we conducted experiments at other temperatures of the ionization chamber and compared these data with those in Fig. 3. The curves $[m^*]/[P^-]$ and $[D^-]/[P^-]$ for $C_{60}F_{36}$ and $C_{60}F_{48}$,[2] obtained at different temperatures of the ionization chamber (solid lines) and calculated model curves for these temperatures (dotted lines) are shown in Fig. 4. As expected by the statistical model, the change in temperature (*i.e.*, the internal vibrational energy of molecules) immediately affected the position of the experimental curves $[m^*]/[P^-]$ (Fig. 4, upper panels). However, the position of an above discussed shoulder on the $[D^-]/[P^-]$ curves hardly changed with temperature (including the case of $C_{60}F_{48}$), although the upper section of these curves shows a tendency to the same shift as the model curves (Fig. 4, lower panels).

Among the most likely reasons of inconsistency of experimental data $[D^-]/[P^-]$ and the results of calculations by the statistical model one could suppose (i) the presence for all three investigated fullerenes of such resonance states in the energy range from 2 to ≈8 eV that would facilitate relatively rapid dissociative decay, which, perhaps, has been terminated still before the complete statistical redistribution of energy among the vibrational degrees of freedom of NI. The temperature independent behavior of the $[D^-]/[P^-]$ curves (see above) could serve as indirect confirmation of this hypothesis. (ii) Taking into account the long lifetime τ_a of fluorofullerene NI, one cannot exclude the possibility of the isomerization of P^- ions prior to fragmentation, for example, *via* migration of the fluorine atoms. Indeed, the so-called "fluorine dance" phenomena were previously shown to accompany the fullerene fluorination reactions [30]. As for NI, fluorine migration is proved to be a rearrangement with comparatively low energy barrier [31], and recently it has found one more evidence for the reverse case, of NI defluorination [32]. Isomerization could lead to more stable isomers, the possible existence of which is indicated by quantum-chemical calculations (see, e.g., Refs. [33,34]). The more stable structure of NI, *ceteris paribus*, means a transition to states with higher internal vibrational energy, corresponding to a higher decay rate constant even if the activation barrier remains constant. Despite the high rates of "extraneous" decay processes under discussion, there is a lot of time for the preliminary structure rearrangements in the molecular ions prior to leaving the ionization chamber, because the ion extraction time t_1 constitutes the tens of microseconds (see Table 1). From general considerations, with the electron energy elevation the simple dissociative processes become more probable, what can explain the better coincidence of experimental and model $[D^-]/[P^-]$ curves at definite energies.

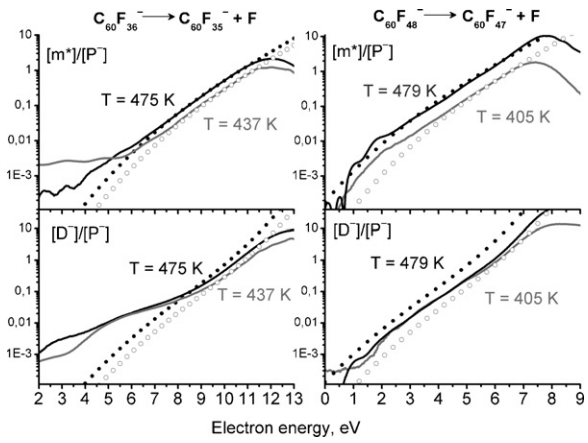

Fig. 4. Experimental (solid lines) and calculated (circles) curves of the energy dependence of intensity relations $[m^*/P^-]$ and $[D^-/P^-]$, obtained at different temperatures of the ionization chamber *T*.

As experience shows, the rearrangement and isomerization processes are rather frequent phenomena for NI of more simple (compared with fullerenes) organic molecules (see, e.g., Refs. [35–39]). For the detection and description of such processes, the thermochemical approach is used based on an analysis of the energy balance of the unimolecular reaction of dissociative decay. For the reaction of dissociative electron capture occurring at threshold all the captured electron energy is presumed to be consumed exclusively for bond dissociation, and therefore the excess energy of the reaction products (translational and electronic or vibrational excitation energy inherited by the charged and neutral fragments) is to be neglected [40]. Thus, minimal (threshold) electron energy sufficient for $C_{60}F_{n-1}^-$ ions to become possible can be theoretically calculated as follows:

$$E_{ap}(C_{60}F_{n-1}^-) = D(C_{60}F_{n-1} - F) - EA(C_{60}F_{n-1}),$$

[2] Extremely high sublimation temperature of $C_{60}F_{18}$ did not allow us to perform such an experiment with this sample.

where E_{ap} is expected appearance energy of the fragment ions, D is C–F bond dissociation energy in a *molecule*, and EA is electron affinity. Knowing the value of $D(C_{60}F_{n-1}{}^{-}F)$ (3.2, 3.06 and 2.98 eV [16]) and taking the $EA(C_{60}F_{n-1})$ values to be 4.285, 4,98 and 5.66 eV [32], we can obtain the energy threshold $E_{ap}(C_{60}F_{n-1}{}^{-})$ to be −1.085, −1.92 and −2.68 eV, respectively, for n = 18, 36 and 48. The obtained appreciably negative values of E_{ap} indicate the extreme exothermicity of the considered dissociative electron capture reactions, implying the absence of any formal energy constraints for the formation of $C_{60}F_{n-1}{}^{-}$ ions even at the capture by $C_{60}F_n$ molecules of electrons with thermal energies. It should be noted, that additional several electronvolts of energy accumulated by the molecules as vibrational internal energy (see Table 1), which is believed to even more facilitate the dissociative electron capture process [40], was not taken into account in above thermochemical considerations. Thus, we cannot confirm or disprove the hypothesis (ii) using the thermochemical approach.

Upon a balance, another question arises: what caused the suppression of dissociative processes (or their very low abundance) at thermal and epithermal energies up to $E_e \approx 2$–3 eV (see Fig. 3a)? In general case the absence of fragment ions in energetically allowed region can be explained by the strong competition from the electron autodetachment process, *i.e.*, by the lack of sufficiently long-lived resonant states in this region (see, *e.g.*, the case of $[M–H]^-$ions from benzene [41] and from polyaromatic compounds [42]). However, as it was shown above, this is not the case for the current objects of investigation. The set of results obtained in present study by using a statistical approach allows us to conclude, that the dissociative processes within the energy range from 0 to 2–3 eV lay beyond the time-window and temperatures of our experiments. Thus, the excess of appearance energy over the calculated energy threshold observed for fragment D^-ions and their later analogues m* should be regarded as a kinetic shift. The term "kinetic shift" in relation to the NI is almost never used but, in our opinion, it is absolutely applicable to the case of fullerenes.

4. Statistical model and calculation method

The statistical model used in this work is described in detail in Ref. [26]. Briefly, the rate constant for unimolecular decay was calculated from the known formula [24]:

$$k(\varepsilon) = \frac{\sigma W^{\pm}(\varepsilon - E_a)}{h\rho(\varepsilon)},$$

where σ is the reaction path degeneracy, E_a is the activation energy, h is the Planck's constant, $W^{\pm}(\varepsilon - E_a)$ is the sum of states of the activated complex in the energy range from 0 to $(\varepsilon - E_a)$, $\rho(\varepsilon)$ is the density of states of the active NI. The $W^{\pm}(\varepsilon)$ and $\rho(\varepsilon)$ functions were calculated using the Stein–Rabinovitch algorithm for harmonic oscillators [43]. For these purposes the vibrational frequencies were calculated for parent ions $C_{60}F_n{}^{-}$ in the assumed symmetry C_{3v}, C_3 and D_3, for n = 18, 36 and 48, respectively [44] at the density functional level of theory (PBE, basis 3z, software package Priroda [45]) with full geometry optimization, and scaled by a factor of 1.02 [44]. Searching the transition state for such a large systems as fullerenes, is a complex and time consuming computational task, so we chose a simplified method of RRKM. Thus, when calculating $W^{\pm}(\varepsilon)$ the stretch of C–F bond in NI was considered as a reaction coordinate (the vibrational mode with a frequency *ca.* 1170 cm^{-1} [44] was excluded); the coefficient σ was equivalent to the number of the C–F bonds (*i.e.*, $\sigma = n$). As a first approximation to the activation energy E_a we have taken from Ref. [16] the calculated enthalpies of reaction (1), *i.e.*, average of the C–F bond energy in the *anion* (in contrast to the expression for the appearance energy E_{ap} (see Section 3) in which the C–F bond dissociation energy for *neutral molecule* was used), constituting 2.59, 2.38, 1.97 eV, respectively, for n = 18, 36 and 48. Later, at fitting the model parameters to obtain the best convergence of the calculations to the experimental data, these values were slightly decreased by 0.07, 0.05 and 0.14 eV, respectively (*cf.* Table 1), which seems reasonable deviation, taken into account nonequivalence of the C–F bonds at different positions in the molecule (ion) of finite symmetry. This feature of the current model is believed to become useful way for rough estimation of the unknown values of bond dissociation energies in negative ions undergoing metastable fragmentation.

The presence of the activation barrier of reverse reaction was disregarded in the calculations, *i.e.*, it was assumed that the kinetic energy of the separated fragments was negligible.

In contrast to Ref. [26], where the internal energy distribution of molecules was simulated by Gaussian function, we have assumed in this paper that the internal vibrational energy of molecules satisfies the Boltzmann distribution [24]:

$$f_M(\varepsilon) = \rho_M(\varepsilon)\exp\left(-\frac{\varepsilon}{kT}\right),$$

where k is the Boltzmann constant, T is the absolute temperature; for the calculation of the density of states $\rho_M(\varepsilon)$ we used the vibrational frequencies of the corresponding *neutral molecules* in the optimal geometries calculated on the base of above described quantum-chemical level of theory.

In the experiment, electrons also possess their own distribution of kinetic energy $\Delta E_{1/2}$ (see Table 1), which in this model is described by a Gaussian function $g(E_e)$; while the model assumed that there is some broadening of the distribution linearly with increasing E_e: $\Delta E_{1/2}(E_e) = \Delta E_{1/2}(0) + a{\cdot}E_e$ [46]. In our calculations, the contribution of electron energy distribution into the NI internal energy distribution was taken into account by the convolution operation with the Boltzmann distribution: $f(\varepsilon) = \int f_M(\varepsilon)\cdot g(\varepsilon - E_e)dE_e$.

We have calculated the number of formed metastable m*, daughter D^-, and parent P^- ions as relations $[m^*]/[P^-]$ and $[D^-]/[P^-]$ using the above-described functions $k(\varepsilon)$ and $f(\varepsilon)$ (see the corresponding equations in Ref. [26]). The time interval t_0–t_1 of ions extraction from the ionization chamber was estimated using numerical simulation of the electric field distribution in the reaction region. The accuracy of this procedure was tested recently by comparison of the calculated extraction time 8.47 μs for the ion m/z = 146 ($SF_6{}^-$) with the experimental data obtained using the same type of instrument as in the present work, and constituting 8.5 ± 1.0 μs [47]. The time of ions' drift in a mass spectrometer t_1–t_4 was evaluated from the known geometrical sizes of the instrument (see Fig. 1) and accelerating potential value. Table 1 presents structural and energetic characteristics of molecules and ions, as well as experimental and other parameters used in this paper for the calculations by the statistical model elaborated.

5. Conclusions

The present mass spectrometric investigation of collisions of low energy (0–20 eV) electrons with the gas-phase targets has revealed the processes of intense resonant electron capture by fluorofullerene molecules $C_{60}F_{18}$, $C_{60}F_{36}$ and $C_{60}F_{48}$ with the formation of long-lived molecular NI. Their main dissociative decay channel is the loss of F atom. The observed metastable nature of the unimolecular decay served as a basis for considering the processes of NI fragmentation from the standpoint of the statistical RRKM theory. The developed simple kinetic model has allowed us to adequately describe the experimental dependences of the decay intensity both on the energy of captured electrons and on the temperature, to explain the suppression of the fragmentation of molecular NI in the region of thermal and epithermal E_e (kinetic shift), as well as to

detect the energy region of fast (possibly non-statistical) fragmentation processes. The results of this investigation extend knowledge of the properties of fullerenes and their derivatives, consistently being inscribed into a set of previously reported phenomena of delayed fragmentation of C_{60}^- NI generated by electron capture [48], and by collisions with atoms [49], a similar observations for positive ions C_{60}^+ [50,51], thermal fragmentation of neutral fullerene molecules (see in Ref. [52]) and the whole family of other phenomena caused by the statistical nature (delayed ionization of molecules [53], collective plasmon excitations [19,20], long lifetimes τ_a of NI [8,23], *etc.*). Data on the behavior of fluorofullerene molecules in a collision with low-energy electrons, obtained in model gas-phase conditions, apart from analytic applications, may be of interest in the development of organic and molecular electronics devices, in particular in the choice of materials and doping agents.

Acknowledgements

The authors would like to express gratitude to O.V. Boltalina for recommendations by the method of injection of fullerenes. This work was supported by Russian Foundation for Basic Research (projects 08-02-97004, 08-02-97010), and Civilian Research and Development Foundation (grant RUC1-2908-UF-07).

References

[1] H. Spanggaard, F.C. Krebs, Solar Energy Mater. Solar Cells 83 (2004) 125.
[2] D.Yu. Paraschuk, A.I. Kokorin, Russ. Chem. J. 52 (2008) 107 (in Russian).
[3] Y.-J. Yu, O. Solomeshch, H. Chechik, A.A. Goryunkov, R.F. Tuktarov, D.H. Choi, J.-I. Jin, Y. Eichen, N. Tessler, J. Appl. Phys. 104 (2008) 124505.
[4] O. Solomeshch, Y.J. Yu, A.A. Goryunkov, L.N. Sidorov, R.F. Tuktarov, D.H. Choi, J.-I. Jin, N. Tessler, Adv. Mater. 21 (2009) 4456.
[5] A.V. Eletskii, B.M. Smirnov, Physics-Uspekhi 38 (1995) 935.
[6] Yu.V. Vasil'ev, R.F. Tuktarov, V.A. Mazunov, Rapid Commun. Mass Spectrom. 11 (1997) 757.
[7] Yu.V. Vasil'ev, O.V. Boltalina, R.F. Tuktarov, V.A. Mazunov, L.N. Sidorov, Int. J. Mass Spectrom. Ion Proc. 173 (1998) 113.
[8] R.F. Tuktarov, R.V. Khatymov, P.V. Shchukin, M.V. Muftakhov, V.Yu. Markov, O.A. Solomeshch, JETP Lett. 90 (2009) 515.
[9] V.I. Khvostenko, Negative Ion Mass Spectrometry of Organic Compounds (Mass spektrometria otritcatelnykh ionov v organicheskoy khimii), Nauka, Moscow, 1981 (in Russian).
[10] V.A. Mazunov, P.V. Shchukin, R.V. Khatymov, M.V. Muftakhov, Mass Spectrom. 3 (2006) 11 (in Russian).
[11] R.V. Khatymov, V.Yu. Markov, R.F. Tuktarov, I.N. Ioffe, M.V. Muftakhov, S.M. Avdoshenko, A.V. Pogulay, L.N. Sidorov, Int. J. Mass Spectrom. 272 (2008) 119.
[12] O.V. Boltalina, V.Yu. Markov, R. Taylor, M.P. Waugh, J. Chem. Soc. Chem. Commun. (1996) 2549.
[13] O.V. Boltalina, A.Ya. Borschevskii, L.N. Sidorov, J.M. Street, R. Taylor, J. Chem. Soc. Chem. Commun. (1996) 529.
[14] O.V. Boltalina, L.N. Sidorov, V.F. Bagryantsev, V.A. Seredenko, A.S. Zapolskii, J.M. Street, R. Taylor, J. Chem. Soc., Perkin Trans. 2 (1996) 2275.
[15] R.G. Cooks, J.H. Beynon, R.M. Caprioli, G.R. Lester, Metastable Ions, Elsevier Scientific publishing, Amsterdam, 1973.
[16] A.V. Streletskii, I.N. Ioffe, S.G. Kotsiris, M.P. Barrow, T. Drewello, S.H. Strauss, O.V. Boltalina, J. Phys. Chem. A 109 (2005) 714.
[17] R.V. Khatymov, R.F. Tuktarov, A.V. Pogulay, M.V. Muftakhov, Russ. J. Phys. Chem. B 3 (2009) 770.
[18] G. Gigli, S. Nunziante Cesaro, J.V. Rau, I.V. Goldt, V.Yu. Markov, A.A. Goryunkov, A.A. Popov, O.V. Boltalina, L.N. Sidorov, in: D.M. Guldi (Ed.), Proceedings—Electrochemical Society, vol. 13, Fullerenes and Nanotubes, Electrochemical Society, Pennington, NJ, 2003, p. 453.
[19] R.F. Tuktarov, R.F. Akhmetyanov, E.S. Shikhovtseva, Yu.A. Lebedev, V.A. Mazunov, JETP Lett. 81 (2005) 171.
[20] R.F. Akhmetyanov, E.S. Shikhovtseva, G.S. Lomakin, Phys. Solid State 51 (2009) 2557.
[21] C. Lifshitz, A.M. Peers, R. Grajower, M. Weiss, J. Chem. Phys. 53 (1970) 4605.
[22] E. Illenberger, B.M. Smirnov, Physics-Uspekhi 41 (1998) 651.
[23] Y.V. Vasil'ev, R.R. Abzalimov, S.K. Nasibullaev, T. Drewello, Fullerene, Nanotubes, and Carbon Nanostructures 12 (2004) 229.
[24] H. Eyring, S.H. Lin, S.M. Lin, Basic Chemical Kinetics, John Wiley, Chichester, NY, 1980.
[25] J.C. Lorquet, Int. J. Mass Spectrom. 200 (2000) 43.
[26] P.V. Shchukin, M.V. Muftakhov, R.V. Khatymov, A.V. Pogulay, Int. J. Mass Spectrom. 273 (2008) 1.
[27] T. Baer, P.M. Mayer, J. Am. Soc. Mass Spectrom. 8 (1997) 103.
[28] K. Vekey, J. Mass Spectrom. 31 (1996) 445.
[29] R.V. Khatymov, M.V. Muftakhov, V.A. Mazunov, Rapid Commun. Mass Spectrom. 17 (2003) 2327.
[30] A.A. Gakh, A.A. Tuinman, Tetrahedron Lett. 42 (2001) 7137.
[31] A.M. Avdoshenko, I.N. Ioffe, L.N. Sidorov, J. Phys. Chem. A 113 (2009) 10833.
[32] X.-B. Wang, C. Chi, M. Zhou, I.V. Kuvychko, K. Seppelt, A.A. Popov, S.H. Strauss, O.V. Boltalina, L.-S. Wang, J. Phys. Chem. A 114 (2010) 1756.
[33] N. Matsuzawa, T. Fukunaga, D.A. Dixon, J. Phys. Chem. 96 (1992) 10747.
[34] J. Cioslowski, N. Rao, A. Szarecka, K. Pernal, Mol. Phys. 99 (2001) 1229.
[35] M.V. Muftakhov, R.V. Khatymov, P.V. Shchukin, A.V. Pogulay, V.A. Mazunov, J. Mass Spectrom. 45 (2010) 82.
[36] R.V. Khatymov, M.V. Muftakhov, V.A. Mazunov, D.V. Nedopekin, I.V. Galyautdinov, V.N. Odinokov, Russ. Chem. Bull. 51 (2002) 306.
[37] R.V. Khatymov, M.V. Muftakhov, P.V. Schukin, V.A. Mazunov, Russ. Chem. Bull. 52 (2003) 1974.
[38] D. Ponomarev, V. Takhistov, J. Mol. Struct. 784 (2006) 177.
[39] D. Ponomarev, V. Takhistov, J. Mol. Struct. 784 (2006) 198.
[40] H.S.W. Massey, Negative Ions, 3rd ed., Cambridge Univ. Press, Cambridge, England, 1976 (translated into Russian, Izd. Mir, 754 pp.).
[41] M.V. Muftakhov, R.V. Khatymov, V.A. Mazunov, Rapid Commun. Mass Spectrom. 14 (2000) 1468.
[42] S. Denifl, S. Ptasinska, B. Sonnweber, P. Scheier, D. Liu, F. Hagelberg, J. Mack, L.T. Scott, T.D. Märk, J. Chem. Phys. 123 (2005) 104308.
[43] S.E. Stein, B.S. Rabinovitch, J. Chem. Phys. 58 (1973) 2438.
[44] J.V. Rau, S.N. Cesaro, O.V. Boltalina, V. Agafonov, A.A. Popov, L.N. Sidorov, Vib. Spectrosc. 34 (2004) 137.
[45] D.N. Laikov, Chem. Phys. Lett. 281 (1997) 151.
[46] V. Grill, H. Drexel, W. Sailer, M. Lezius, T.D. Mark, Int. J. Mass Spectrom. 205 (2001) 209.
[47] V.G. Lukin, G.S. Lomakin, Instrum. Exp. Techn. 53 (2010) 401.
[48] A. Bekkerman, B. Tsipinyuk, E. Kolodney, Int. J. Mass Spectrom. Ion Proc. (1999) 773, 185/186/187.
[49] R.F.M. Lobo, N.T. Silva, B.M.N. Vicente, I.M.V. Gouveia, F.M.V. Berardo, J.H.F. Ribeiro, Eur. Phys. J. D 38 (2006) 35.
[50] M. Foltin, M. Lezius, P. Scheier, T.D. Mark, J. Chem. Phys. 98 (1993) 9624.
[51] C. Lifshitz, Int. J. Mass Spectrom. 198 (2000) 1.
[52] L.A. Openov, A.I. Podlivaev, JETP Lett. 84 (2006) 68.
[53] E.E.B. Campbell, R.D. Levine, Annu. Rev. Phys. Chem. 51 (2000) 65.